tained from the neutral interchange reactions. Since the concentrations of $O_2^+ \cdot N_2$ and $O_2^+ \cdot H_2$ obtained in the present experiments were extremely small, due to their rapid reaction with O_2, it was not possible to measure their reactions. However, from the termolecular association reactions producing these ions it has been found that $p\tau$ is smaller for the $(O_2^+ \cdot H_2)^*$ intermediate complex than for the $(O_2^+ \cdot N_2)^*$ intermediate complex. If it is assumed that τ_0 and p are similar for the two cases and since s is likely to be the same, then $O_2^+ \cdot N_2$ is believed to be more strongly bound than $O_2^+ \cdot H_2$.

The relative bond energies of neutrals attached to O_2^+ are in general agreement with simple electrostatic energy calculations using molecular polarizabilities, dipole moments, and sizes, except for O_4^+ which is known to have too large a bond energy[5] to fit a simple model. It can be seen from Table VI that the order of the dissociation energies is identical for O^- and O_2^- ions clustered with molecules which are present in both sequences.

ACKNOWLEDGMENTS

This work has been supported in part by the Defense Atomic Support Agency. One of us (N.G.A.) wishes to acknowledge the European Space Research Organization for the provision of financial support.

* NASA International University Fellow. Present address: Electron Physics Department, University of Birmingham, England.

† NRC of U.S. Postdoctoral Research Associate. Present address: Department of Chemistry, York University, Toronto, Canada.

[1] D. B. Dunkin, F. C. Fehsenfeld, A. L. Schmeltekopf, and E. E. Ferguson, J. Chem. Phys. **49**, 1365 (1968).

[2] A. Good, D. A. Durden, and P. Kebarle, 17th Annual Conference on Mass Spectrometry and Allied Topics, Dallas, Texas, May 1969. See also J. Chem. Phys. **52**, 212, 222 (1970).

[3] P. Kebarle, S. K. Searles, A. Zolla, T. Scarborough, and M. Arshadi, J. Am. Chem. Soc. **89**, 6393 (1967).

[4] For example, R. H. Fowler and E. A. Guggenheim, *Statistical Thermodynamics* (Cambridge University Press, Cambridge, England, 1952), p. 497.

[5] J. H. Yang and D. C. Conway, J. Chem. Phys. **40**, 1729 (1964).

[6] J. L. Pack and A. V. Phelps, J. Chem. Phys. **45**, 4316 (1966).

[7] D. C. Conway and L. E. Nesbitt, J. Chem. Phys. **48**, 509 (1968).

[8] P. Warneck, Chem. Phys. Letters **3**, 532 (1969).

[9] E. F. Hayes and G. V. Pfeiffer, J. Am. Chem. Soc. **90**, 4773 (1968).

[10] F. C. Fehsenfeld, E. E. Ferguson, and D. K. Bohme, Planetary Space Sci. **17**, 1759 (1969).

[11] D. K. Bohme, D. B. Dunkin, F. C. Fehsenfeld, and E. E. Ferguson, J. Chem. Phys. **50**, 863 (1969).

[12] G. Gioumousis and D. P. Stevenson, J. Chem. Phys. **29**, 294 (1958).

[13] H. S. Johnston, *Gas Phase Reaction Rate Theory* (Ronald Press, New York, 1966).

[14] D. A. Durden, P. Kebarle, and A. Good, J. Chem. Phys. **50**, 805 (1969).

[15] E. E. Ferguson, Can. J. Chem. **47**, 1815 (1969).

THE JOURNAL OF CHEMICAL PHYSICS VOLUME 52, NUMBER 6 15 MARCH 1970

Rotational–Translational Energy Transfer. II. Comparison of Action-Angle Solution in the Near-Static Approximation with Exact Results*

AUDREY O. COHEN† AND R. A. MARCUS

Noyes Chemical Laboratory, University of Illinois, Urbana, Illinois 61801

(Received 26 September 1969)

In Part I, the differential equations for molecular rotational–vibrational–translational energy transfer were re-expressed in terms of action-angle variables. In the present paper, approximate integral solutions and exact results for rotational–translational transfer are compared for a wide range of collisional and molecular parameters at small fractional changes in translational energy. The results are in good agreement over the range investigated except at low moments of inertia. Thereby, conditions where the present approximation is best correspond to some which are least accessible by approximate or numerical quantum mechanical methods. The present approximation employs for zeroth order a classical analog of the static approximation in quantum mechanics, rather than the adiabatic approximation, and the results have implications for the ranges of molecular parameters where each should be preferable in the quantum case.

INTRODUCTION

In Part I[1] it was shown that the classical mechanical differential equations for rotational–translational–vibrational energy transfer in molecular collisions could be usefully transformed into differential equations for action-angle variables. Integration of the latter equations yields directly the change in quantities such as rotational angular momentum j, its z component m_j, etc. Since the action variables frequently vary only slowly during a collision, the new exact differential equations are easier to integrate than the original ones.

Several approximations can be introduced into the equations. In the present paper, the approximate results are compared with exact ones obtained from numerical integration of the original equations of motion, for the case of an atom colliding with a rigid linear molecule. The results permit an analysis, via semiclassical arguments, of various approximations in quantum treatments of phenomena involving rotational–translational energy transfer.[2]

The change in rotational angular momentum **j** can be calculated directly or, from the change in orbital angular momentum **l**, indirectly. Both methods are

employed and compared in the present paper. Comparison of exact and approximate results is made for various impact parameters, **j**'s, **l**'s, rotational and orbital phases, and for various molecular parameters. In particular, the effect of varying the repulsive and attractive asymmetry parameters in a 6–12 potential is considered. Comparisons are also made for several specific molecular systems.

DIRECT CALCULATION OF Δj

The space-fixed coordinate system in Fig. 1 is used for the direct calculation of Δj. The rotator is described in terms of its action variables $(2\pi j, 2\pi m_j)$ and the conjugate angle variables $(\psi/2\pi, \beta_{m_j}/2\pi)$, where j and m_j are the rotational angular momentum and its z component and where ψ and β_{m_j} are given in Fig. 1. [The usual polar coordinates (θ, ϕ) of the rotator are related to these variables via Eq. (23) of Part I.] The initial orbital plane of the elastic collision will be chosen to be the xy plane. [Thereby, initially, $\Theta=\frac{1}{2}\pi$ in Eq. (22) of Part I.]

Various approximations can be introduced into Hamilton's equations for the rate of change of the above action-angle variables of the rotator and for the variables describing the relative translational motion, for example, the following:

1. The variables of relative motion (R, Θ, Φ) and their conjugate momenta on the right-hand sides of these equations are replaced by their elastic collision values, and six coupled equations of motion are integrated numerically.[3]

2. (a) All variables on the right-hand sides are replaced by their elastic collision values, reducing the problem to the evaluation of integrals; (b) the components of Δ**j** are calculated, and Δj obtained from them; (c) an iteration based on (a) is used; (d) in addition to (a)–(c), symmetrization of initial and final translational velocities is used, so as to satisfy microscopic reversibility.[4]

Approximation 1 is the low-mass approximation of Cross and Herschbach,[5] expressed now in terms of action-angle coordinates for the rotator. The approximations in 2(a)–2(c) are the principal ones used in the present paper. It is shown later (Appendices A plus C) that 2(b) represents a partial contribution to 2(c). The computer time for approximation 1 is approximately the same as that for solving the exact (all 10) coupled equations of motion. For that reason, the principal value of 1 lies in the physical insight it provides when a comparison with exact results is made.

Symmetrization 2(d) can be omitted in the present paper since the initial conditions employed lead to a low fractional change in translational energy. The latter condition, which is commonly assumed in approximate theories of line broadening,[6] is also relevant to many other phenomena which concentrate on small $|\Delta j|$.[7]

When approximation 1 is made for the relative motion

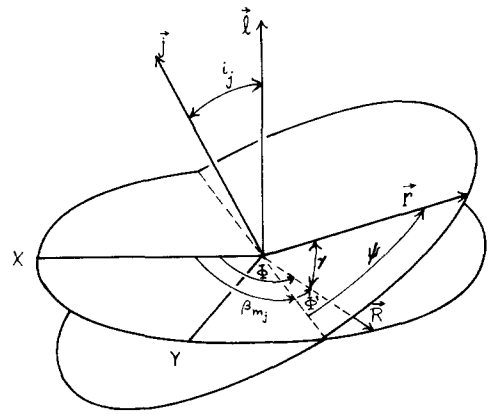

FIG. 1. Coordinate system used for the direct calculation of changes in components of **j**.

the orbital plane for the elastic collision is the same as the initial orbital plane, i.e., the xy plane in Fig. 1. From Eqs. (21) and (26) of Part I (setting $\Theta=\frac{1}{2}\pi$) one then finds

$$dj/dt=F(\gamma, t)[\cos i_j \cos\psi \sin\Phi'-\sin\psi \cos\Phi'], \quad (1)$$

$$dm_j/dt=F(\gamma, t)[-\cos i_j \sin\psi \cos\Phi'+\cos\psi \sin\Phi'], \quad (2)$$

$$d\psi/dt=F(\gamma, t)j^{-1}\cos i_j \sin\psi \sin\Phi'+j/I, \quad (3)$$

$$d\beta_{m_j}/dt=-F(\gamma, t)j^{-1}\sin\psi \sin\Phi', \quad (4)$$

where I is the moment of inertia, i_j, γ, and Φ' are the angles (Fig. 1) between **j** and the z axis, between the rotor axis **r** and the line of centers **R**, and between the line of nodes and the line of centers of the two colliding particles, respectively. In Eqs. (1)–(4) we have

$$\cos i_j=m_j/j, \quad (5)$$

$$\cos\gamma=\cos i_j \sin\psi \sin\Phi'+\cos\psi \cos\Phi', \quad (6)$$

$$\Phi'=\Phi-\beta_{m_j}. \quad (7)$$

$F(\gamma, t)$ is given by

$$F(\gamma, t)=-\partial V_p(R, \cos\gamma)/\partial \cos\gamma, \quad (8)$$

where V_p is the anisotropic part of the interaction potential V,

$$V_p=V-\frac{1}{2}\int_0^\pi V \sin\gamma d\gamma. \quad (9)$$

Without loss of generality the distance of closest approach in the elastic collision may be taken to occur at $t=0$. The elastic collision values for ψ and Φ' are

$$\psi=(jt/I)+\delta_\psi=\omega t+\delta_\psi, \quad (10)$$

$$\Phi'=\int_0^t \frac{l_0}{\mu R^2}dt+\delta_{\Phi'}, \quad (11)$$

where δ_ψ and $\delta_{\Phi'}$, the values of these angles at $t=0$, occur randomly in $(0, 2\pi)$. ω is the rotational angular fre-

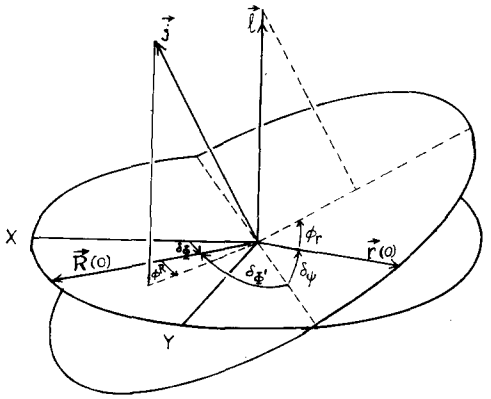

FIG. 2. Phases ϕ^R and ϕ^r indicating midpoint orientations of the line of centers and rotor, respectively, for an elastic collision.

quency. $R(t)$ obeys (12),

$$t=\int_{R_{\min}}^{R}\left(\frac{2[E-V_0-E_{\rm rot}-(l_0^2/2\mu R^2)]}{\mu}\right)^{-1/2}dR, \quad (12)$$

where V_0 is the spherically averaged value of V [the second term in Eq. (9)]. $E_{\rm rot}$ and l_0 are the initial rotational energy of the linear molecule and the initial orbital angular momentum, respectively.

Approximation 2(a) is made for the rotational motion by replacing i_j and β_{m_j} in Eqs. (1)–(4) by their initial values and by using the elastic collision value for ψ. The resulting value for Δj, which for reasons discussed later will be denoted by $\Delta j^{\parallel}$, is (13), where ψ and Φ' are given by (10) and (11):

$$\Delta j^{\parallel}=\int_{-\infty}^{\infty}F(\gamma,t)[\cos i_j\cos\psi\sin\Phi'-\sin\psi\cos\Phi']dt. \quad (13)$$

When $F(\gamma,t)$ and (6) are introduced into (13) and the trigonometric addition laws for the various sines and cosines are applied, the $\cos i_j$, the $\sin\delta$'s, and $\cos\delta$'s can be placed outside the integrals. The asymmetry parameters a also appear outside the integrals. Thus, once the integrals are evaluated for a set of initial conditions they have been evaluated for all δ's, all i_j's, and all a's.

In Appendix A it is shown that approximation 2(b) yields

$$\Delta j=[(j_0+\Delta j^{\parallel})^2+(\Delta j^{\perp})^2]^{1/2}-j_0, \quad (14)$$

where $\Delta j^{\parallel}$ is defined by (13) and $(\Delta j^{\perp})^2$ by

$$(\Delta j^{\perp})^2=\sin^2 i_j\left[\left(\int_{-\infty}^{\infty}F(\gamma,t)\sin\Phi'\cos\psi dt\right)^2+\left(\int_{-\infty}^{\infty}F(\gamma,t)\sin\Phi'\sin\psi dt\right)^2\right]. \quad (15)$$

In Appendix C it is shown that an approximation which is complete through second order (in an expression for j^2) in its allowance for the change of orientation of the rotational plane during collision is given by an equation [Eq. (C7)] similar to (14) with one additional second-order term included under the radical sign. The influence of the latter is minor and is discussed later.

If (14) were expanded it would yield

$$\Delta j\cong\Delta j^{\parallel}+(\Delta j^{\perp})^2/2j_0. \quad (16)$$

Thus, only $\Delta j^{\parallel}$ contributes to the first-order term, making it clear why $\Delta j^{\perp}$ was not obtained in the first-order calculation (13) for the change in magnitude of j.

Equation (14) would have been an exact equation, simple vector arguments show, if $\Delta j^{\parallel}$ and $\Delta j^{\perp}$ had denoted the exact components of $\Delta\mathbf{j}$ parallel to and perpendicular to $\mathbf{j}_0$. Instead, (13) and (15) actually represent approximations to these components (Appendix A), thus motivating the notation.

The exact (numerical) results for Δj will be compared[8] with (14) and with its first-order contribution (13).

It will be convenient to introduce two phases ϕ^R and ϕ^r, as in Fig. 2. ϕ^R and ϕ^r are the angles which the projection of $\mathbf{j}$ on the orbital plane and which the projection of $\mathbf{l}$ on the rotational plane make with the line of centers $\mathbf{R}(0)$ and with the rotor axis $\mathbf{r}(0)$, respectively, at the midpoint of the elastic collision, with signs indicated by Fig. 2. The phases δ_ψ and $\delta_{\Phi'}$ of the direct calculation are related to ϕ^r and ϕ^R by (17), as one sees from Fig. 2,

$$\delta_\psi=\tfrac{1}{2}\pi-\phi^r, \qquad \delta_{\Phi'}=-\tfrac{1}{2}\pi-\phi^R. \quad (17)$$

INDIRECT CALCULATION OF Δj

In this case the change in components of $\mathbf{l}$ is calculated, and $\Delta\mathbf{j}$ is then obtained from angular momentum conservation. It is convenient to use the space-fixed coordinate system given in Fig. 3, which is similar to Fig. 1 but with the orbital and rotator planes inter-

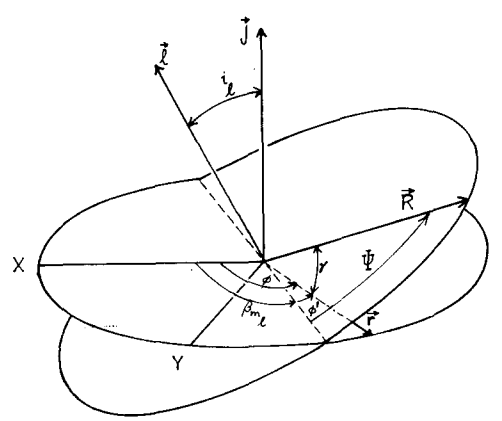

FIG. 3. Coordinate system used for the indirect calculation of Δj.

TABLE I. Parameters and conditions for figures.[a]

Figure	b	I	E^R	E^r	i	ϕ^R	ϕ^r	a_2
4	...	...	...	...	...	$\pi/3$	$o-\pi$	...
5	...	...	...	...	...	$o-\pi$	$\pi/6$	...
6	...	...	...	...	$o-\pi$	...	$2\pi/9$	...
7	...	...	...	...	...	...	...	0.1–0.9
8	0.1–2	$\frac{2}{3}$, 0.1[b]	...	0.25, 2[b]	...	...	...	...
9	0.4, 1	...	0.5–5	...	...	...	...	...
10	0.1, 1	...	...	0–80	...	-0.145π	...	...
11	...	$10^{-2}-1$	...	2	...	-0.145π	...	...
12	...	0.005–3	...	...	...	-0.145π	...	...
13	...	$10^{-3}-1$	...	I[c]	...	...	$\pi/3$	...
14	...	$10^{-3}-1$	...	$10I$	...	...	$\pi/3$	...
15	...	$10^{-3}-1$	...	$100I$	...	...	$\pi/3$	...
16	0.1–2	...	...	...	...	...	...	See Fig.
17	...	0.0024	1.65	0.0064–1.85	...	$-\pi/3$	$-\pi/2$	0.11
18.	...	0.0685	7.86	0.0121–10.2	...	$-\pi/3$	$-\pi/2$	0.18
19	...	0.392	1.39	$4\times10^{-5}-1.9$	...	$-\pi/3$	$-\pi/2$	0.22
20	0.1–2	...	...	...	...	...	...	...

[a] Unless otherwise stated the conditions are $b=1$, $I=\frac{2}{3}$, $E^R=3$, $E^r=0.2483$, $i_j=\pi/4$, $\phi^R=\pi/6$, $\phi^r=3\pi/2$, $a_2=0.3$.

[b] When $E^r=0.25$, $I=\frac{2}{3}$; when $E^r=2$, $I=0.1$, in Fig. 8.

[c] In Figs. 13–15, to keep ω constant, E^r was varied as I was varied.

changed. The angle-action orbital coordinates of the former are $2\pi l$, $2\pi m_l$, $\Psi/2\pi$, and $\beta_{m_l}/2\pi$. The xy plane in Fig. 3 is chosen to be the initial rotational plane. As in the direct calculations various aproximations can be introduced:

1. The four rotator variables on the right-hand sides of the equations of motion are replaced by their elastic collision values, and six coupled equations of motion are integrated numerically.

2. (a) All variables on the right side of the equations of motion are replaced by their elastic collision values, and the components of Δj then calculated from those of Δl; (b) some iteration and/or symmetrization is used.

Approximation 1 is the flywheel approximation of Cross and Herschbach[5] and, once again, its principal and considerable virtue lies in the physical insight provided by a comparison of its results with the exact ones. Approximation 2(a) is the subject of the present section. The equations of motion for the orbital properties are similar to (1)–(4), but with j, m_j, ψ, β_{m_j}, Φ', i_j, β_{m_j} replaced by l, m_l, Ψ, β_{m_l}, $\phi-\beta_{m_l}$, i_l, β_{m_l}, respectively. However, $R(t)$ is again given by (12). We have

$$\Delta j=[(\Delta l_x)^2+(\Delta l_y)^2+(j_0-\Delta m_l)^2]^{1/2}-j_0 \quad (18)$$

since the initial value of (j_x, j_y, j_z) was $(0, 0, j_0)$ in Fig. 3. In Appendix B it is shown that the calculation of Δl_x, Δl_y, and Δm_l and the use of (18) yields (in admittedly a slightly simpler manner) the result already obtained in (14), (13), and (15) so that we need not consider approximation 2(a) further. [Nor will 2(b) be considered.]

RESULTS

The potential used for simplicity in the comparison of exact and approximate results is a Lennard-Jones one with a $P_2(\cos\gamma)$ asymmetry, though the preceding formulations permit, of course, any potential function:

$$V=4\epsilon[(R/\sigma)^{-12}-(R/\sigma)^{-6}]+V_p, \quad (19)$$

$$V_p=4\epsilon(R/\sigma)^{-12}a_R P_2(\cos\gamma)-4\epsilon(R/\sigma)^{-6}a_A P_2(\cos\gamma). \quad (20)$$

In the comparison below, all energies are expressed in units of ϵ, distances in units of σ, and masses in units of μ, the reduced mass of the colliding pair. The angular momenta are then in units of $(\sigma^2\mu\epsilon)^{1/2}$. The impact parameter, in units of σ, is denoted by b. The moment of inertia of the rotator in units of $\mu\sigma^2$ is denoted by I, and the initial translational and rotational energy in units of ϵ by E^R and E^r, respectively. The dimensionless variables defining the system are b, I, E^R, E^r, i, ϕ^R, ϕ^r, and the a's; i is the initial angle between **j** and **l**, and ϕ^R and ϕ^r are the orbital and rotational phases in the elastic collision (Fig. 2). The initial angular momenta are related to the energies E^R and E^r by $l=b(2E^R)^{1/2}$ and $j=(2IE^r)^{1/2}$.

The effect of varying each of these properties was studied. In many of the results the standard set of conditions from which variations were explored was $b=1$, $I=\frac{2}{3}$, $E^R=3$, $E^r\cong0.25$, $i=\frac{1}{4}\pi$, $\phi^R=\frac{1}{6}\pi$, and $\phi^r=\frac{3}{2}\pi$. The detailed conditions for each of the figures are listed in Table I. In most of the cases $l_0\gg j_0$ since $E^R\gg E^r$ and $I\cong b^2$. However, in Fig. 10, E^r was varied from 0–80, and appreciable values of E^r occur in portions of Figs. 8,

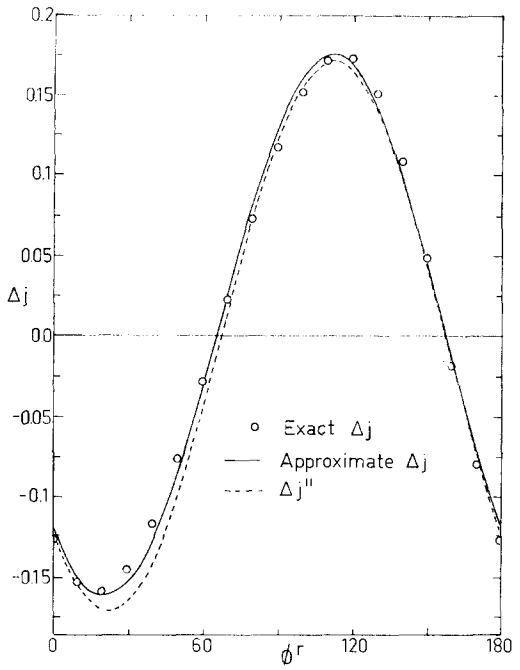

FIG. 4. Angular momentum transfer as a function of the phase of the rotor.

13–15, 17–19, and in 11 (cf. Table I). The method of performing the exact calculations is indicated in Appendix D.

In Fig. 4 the approximation Δj, the $\Delta j^{\parallel}$ and exact Δj are compared versus rotational phase ϕ^r, in Fig. 5 versus orbital phase ϕ^R, and in Fig. 6 versus initial (j, l) angle, i_j.

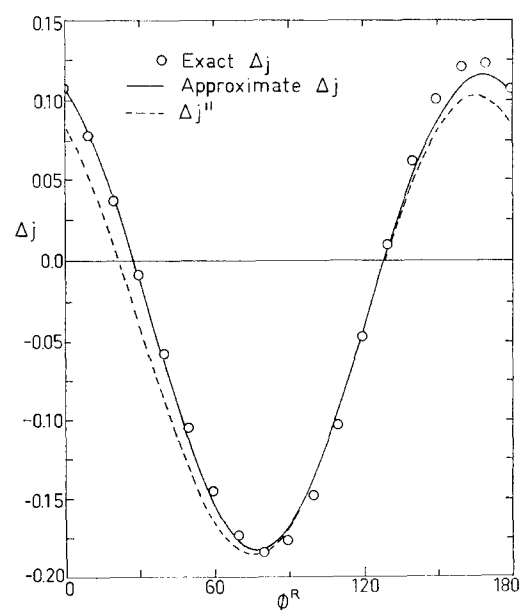

FIG. 5. Angular momentum transfer as a function of the phase of the line of centers.

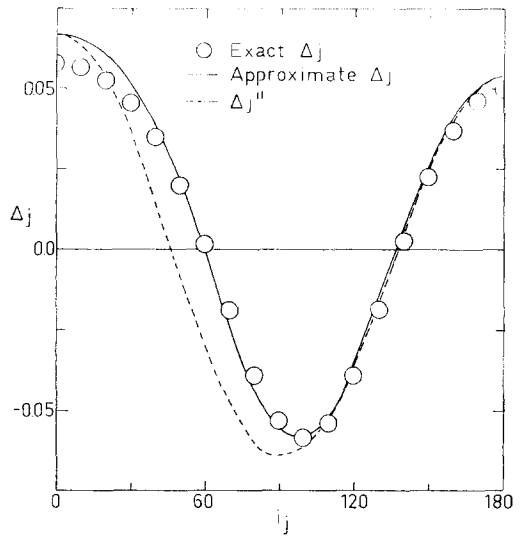

FIG. 6. Angular momentum transfer as a function of the initial angle between I and j.

In Fig. 7 the comparison is made versus asymmetry parameter a_2 ($a_A = a_R = a_2$). According to Eq. (13) the $\Delta j^{\parallel}$ is linear in a_2 but, as seen from (14), Δj has an additional quadratic component (cf. Fig. 7). In Fig. 8, a comparison is made versus reduced impact parameter b. The decrease at large b is due to decreased interaction.

In Fig. 9, a comparison is made versus initial relative translational energy E^R. Δj tends to decrease with increasing E^R in Fig. 9, reminiscent of the similar behavior in many other collision processes at high

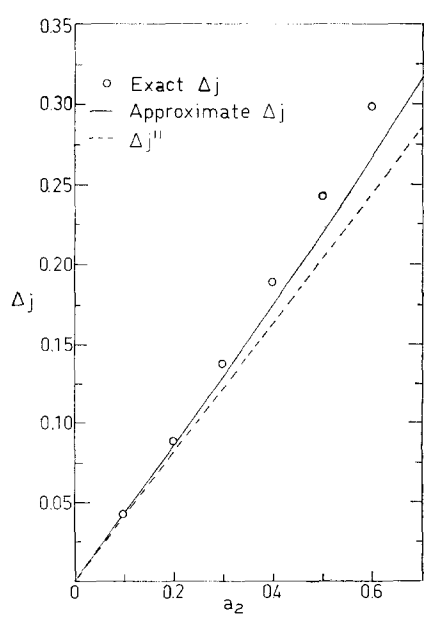

FIG. 7. Angular momentum transfer as a function of the asymmetry parameter a_2. ($a_- = a_A = a_R$).

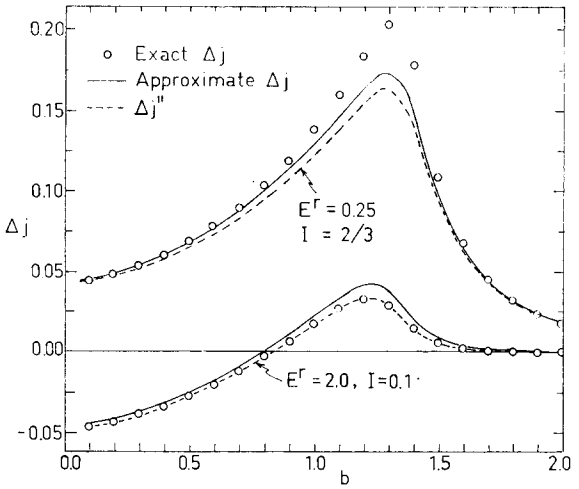

FIG. 8. Angular momentum transfer as a function of impact parameter for a slowly rotating molecule $[\omega=(0.75)^{1/2}]$ and for a more typical rotating one $[(\omega=(40)^{1/2}]$. Here, angular frequency $\omega[=(2E^r/I)^{1/2}]$ is in units of $(\epsilon/\mu\sigma^2)^{1/2}$ radians.

relative velocity $\dot{R}$. This result is understood by noting that the rotator phase (ψ in Fig. 1 and ϕ in Fig. 3) varies little during the collision, under the conditions of Fig. 9 and of many other figures. We transform dt in (13) to $dR/\dot{R}$ and write $\dot{R}$ in terms of E^R and b, as in Ref. 3, where $E-E_{\rm rot}=E^R$ and $l_0^2=2E^Rb^2$. The remaining factors in the integrand now depend mainly on R, and the reason for an inverse dependence (at small ω) of Δj on E^R becomes clear. At high ω ($\omega\gg l_0/b^2$, the "orbital frequency") Δj would be expected to *increase* initially with increasing E^R.

In Fig. 10 a comparison is made versus initial rotational energy E^r and hence with increasing rotational frequency ω. At high enough E^r an increased ω leads to a decreasing Δj, shown by applying the Riemann-Lebesque lemma[9] to Eq. (13) and noting that the second-order term in (16) becomes negligible at large enough j_0. At low E^r the $\Delta j^{\rm II}$ given by (13) should tend to a constant since the rotator phase is only slowly

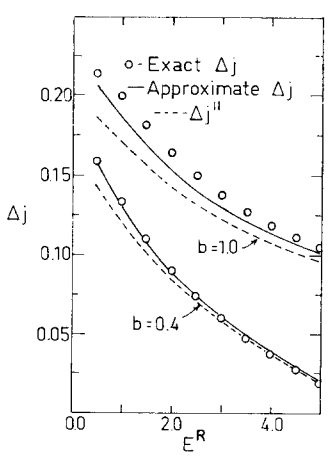

FIG. 9. Angular momentum transfer as a function of initial relative translational energy at a low impact parameter ($b=0.4$) and at an intermediate one ($b=1.0$).

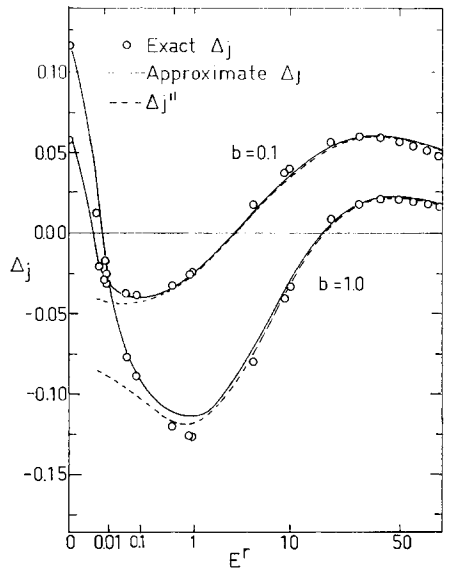

FIG. 10. Angular momentum transfer as a function of initial rotational energy at a low impact parameter ($b=0.1$) and at an intermediate one ($b=1.0$). Values of E^r are plotted on a fourth-root scale. Values of approximate Δj at $E^r=0$ were obtained by extrapolating Δl from higher values of E^r and, apart from sign, taking $\Delta j=|\Delta \mathbf{j}|=|\Delta \mathbf{l}|$ at $E^r=0$.

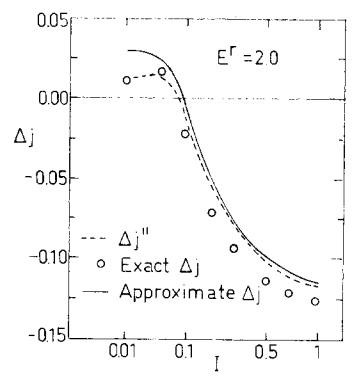

FIG. 11. Angular momentum transfer as a function of the moment of inertia of the rotor at a low initial rotational energy. Values of I are plotted on a cube-root scale.

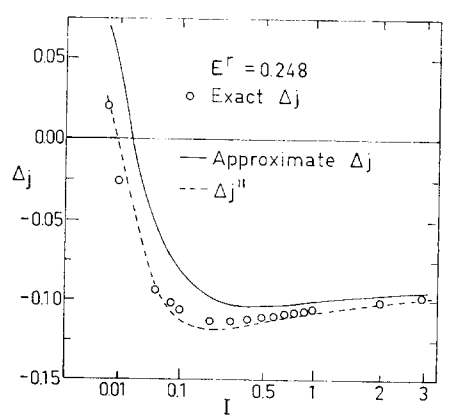

FIG. 12. Angular momentum transfer as a function of the moment of inertia of the rotor at a moderate initial rotational energy. Scale is the same as in Fig. 11.

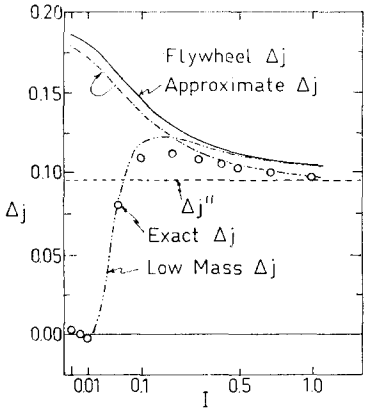

FIG. 13. Angular momentum transfer as a function of the moment of inertia of the rotor at a constant low angular velocity of rotation. Values of I are plotted on a square-root scale.

TABLE II. Reduced moments of inertia[a] I.

	He	Ne	Ar	Kr	Xe
H_2	0.027	0.0184	0.0142	0.0131	0.0114
HI	0.059	0.0120	0.0059	0.0037	0.0024
HCl	0.050	0.0130	0.0073	0.0051	0.0041
N_2	0.24	0.069	0.040	0.030	0.021
CO	0.26	0.073	0.043	0.032	0.026
O_2	0.36	0.098	0.056	0.040	0.032
HC≡CH	0.37	0.102	0.062	0.047	0.039
N_2O	1.05	0.26	0.144	0.099	0.078
CO_2	1.10	0.28	0.156	0.110	0.087
Cl_2	1.55	0.36	0.183	0.116	0.088
CS_2	3.28	0.74	0.38	0.24	0.178
Br_2	4.53	0.91	0.44	0.24	0.172
I_2	8.1	1.58	0.74	0.39	0.26

[a] The moment of inertia of linear molecule divided by the $\mu\sigma^2$ for its collision with an atom. The I's were calculated from data in J. O. Hirschfelder, C. F. Curtiss, and R. B. Bird, *Molecular Theory of Gases and Liquids* (John Wiley & Sons, Inc., New York, 1954), pp. 1110–1112; G. Herzberg, *Molecular Spectra and Molecular Structure* (D. Van Nostrand Co., Inc. Princeton, N. J., 1950) Vol. 1, pp. 502–579; and G. Herzberg, *Molecular Spectra and Molecular Structure* (D. Van Nostrand Co., Inc., Princeton, N. J., 1966), Vol. 3, pp. 583–667.

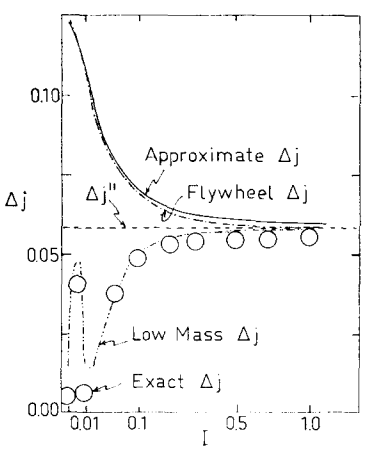

FIG. 14. Angular momentum transfer as a function of the moment of inertia at a constant moderate angular velocity of rotation. Scale for I is the same as in Fig. 13.

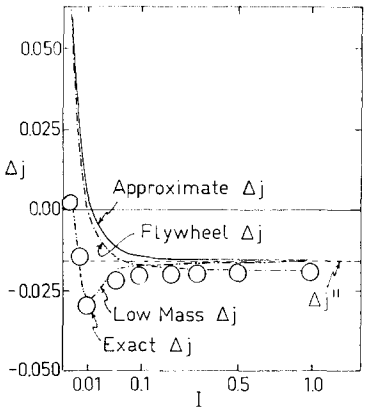

FIG. 15. Angular momentum transfer as a function of the moment of inertia of the rotor at a constant high angular velocity of rotation. Scale for I is the same as Fig. 13.

varying these and no other term in (13) depends on E^r.

In Figs. 11 and 12 a comparison is made versus the reduced moment of inertia I. At sufficiently high I, ω is low and the instantaneous rotator phase is approximately constant during the collision, leading to a Δj independent of I there. At low enough I, ω will tend to infinity and so Δj will eventually vanish.

In Figs. 13–15 a comparison is made versus I at fixed ω. Here $\Delta j^{\parallel}$ and $\Delta j^{\perp}$ are each independent of I [Eqs. (10), (13), and (15)]. However, j_0 is proportional to I at fixed ω, leading at low I to a change of Δj from its

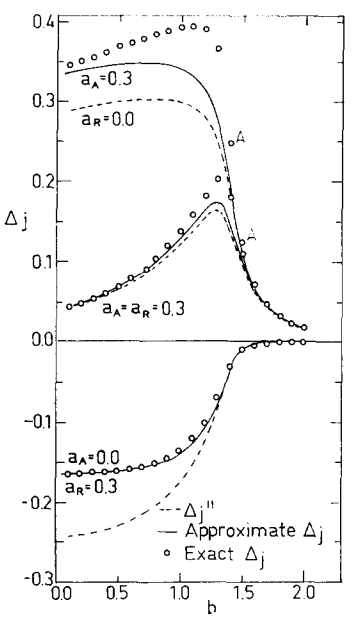

FIG. 16. Angular momentum transfer as a function of impact parameter for three different combinations of attractive and repulsive asymmetry parameters. The upper set of curves (a_A= 0.3, a_R=0.0) is for a purely attractive anisotropic potential, while the lower set of curves (a_A=0.0, a_R=0.3) is for a purely repulsive one. The middle set of curves (a_A=a_R=0.3) is the same set shown in Fig. 8 (E^r=0.25, I=$\frac{2}{3}$). Two of the points belonging to the upper set are labeled A to avoid confusion with the middle set.

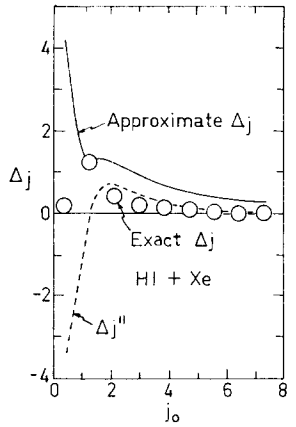

FIG. 17. Angular momentum transfer as a function of initial rotational angular momentum for HI+Xe. The size of the circles indicates the precision of the numerical calculations of all three solutions. For HI+Xe, Δj was multiplied by a conversion factor proportional to $(\mu\sigma^2\epsilon)^{1/2}$, namely 78, to calculate Δj in $\hbar$.

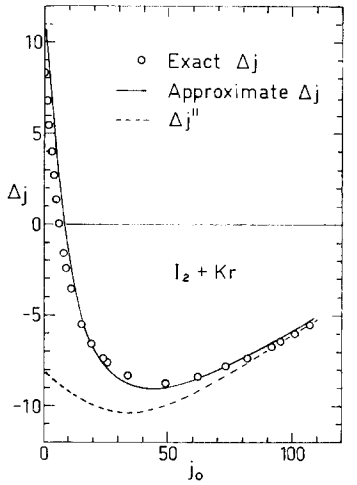

FIG. 19. Angular momentum transfer as a function of initial rotational angular momentum for I_2+Kr. For this figure, a conversion factor of 88 was used to calculate Δj in $\hbar$.

high value. The ω for Fig. 13 is low and since quantization imposes a lower limit on the angular momentum, this low ω is encountered in practice for systems having $I>0.1$. The low-mass and flywheel approximations are also given in Figs. 13–15.

In Fig. 16 a comparison is made versus b for unequal a_A and a_R. At large impact parameters ($b\geq 1.5$) the influence of a_R is negligible, so that most of the preceding curves also apply roughly to the case of small a_R as well (when E^R is not large). When $\Delta j^{\|}$ is a good approximation, one sees from (13) that the effects of the a_A and a_R terms are algebraically additive.

Comparison for several actual molecules is given in Figs. 17–19. Units in Figs. 17–19 are $\hbar$ rather than $(\mu\sigma^2\epsilon)^{1/2}$. The I of $\frac{2}{3}$ used in most of the earlier figures is close to that (0.74) estimated for CS_2+Ne and to that (0.74) estimated for I_2+Ar. An E^R of 3 corresponds to about 0.8 and 1.5 kcal/mole, respectively, for these two molecular systems. To convert the Δj's in Figs. 4–16 to units of $\hbar$ for these two systems one must multiply by about 25 and 60, respectively. Other typical I's are listed in Table II, for comparison with the earlier figures. Asymmetry parameters are summarized in Table III, though the asymmetric force law has usually been assumed rather than established.

Other properties which are of interest in making comparisons of spectral broadening theories and scattering theories with experimental include α, the angle between initial and final **j**. A typical plot is given in Fig. 20.

In Figs. 4–19, Eq. (14) was used to calculate the approximate Δj. Equation (16) would yield results of comparable accuracy for the approximate Δj in these

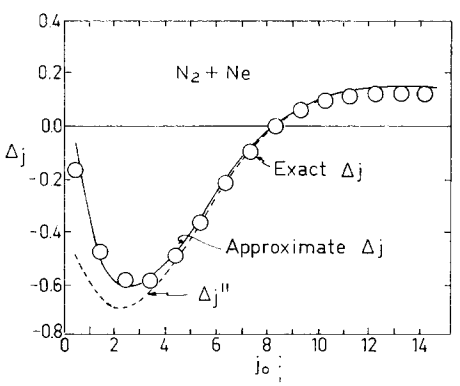

FIG. 18. Angular momentum transfer as a function of initial rotational angular momentum for N_2+Ne. For this figure, a conversion factor of 12 was used to calculate Δj in $\hbar$.

TABLE III. Attractive and repulsive asymmetry parameters.

Molecule	a_A	a_R	References
H_2	0.09, 0.128	0.18, 0.375	a, b, c, d
N_2	0.18, 0.13	0.15	a, b, e
O_2	0.24, 0.23	0.1	a, b, e
Cl_2	0.21, 0.19	···	a, b
HCl	0.09, 0.04, 0.12	<0.61	a, b, f, f
HBr	0.08, 0.06	<0.46	a, f, f
HI	0.11, 0.03	<0.43	a, f, f
N_2O	0.31, 0.33	0.05	a, b, e
CO	0.17, 0.09	0.2, 0.8	a, b, e, g
NO	0.16	0.15, <0.45	b, e, f
CO_2	0.26, 0.27	−0.1	a, b, e
CS_2	0.37	···	a
HCN	0.26	···	a
HC≡CH	0.27, 0.18	0.3	a, b, e
TIF	0.23	···	h

[a] Calculated from polarizability data in J. O. Hirschfelder, C. F. Curtiss, and R. B. Bird, *Molecular Theory of Gases and Liquids* (John Wiley & Sons, Inc., New York, 1954), p. 950.
[b] Anisotropy for 6328 Å from N. J. Bridge and A. D. Buckingham, Proc. Roy. Soc. (London) **295**, 334 (1966).
[c] M. Krauss and F. H. Mies, J. Chem. Phys. **42**, 2703 (1965).
[d] C. S. Roberts, Phys. Rev. **131**, 203, 209 (1963).
[e] J. H. Spurling and E. A. Mason, J. Chem. Phys. **46**, 322 (1967).
[f] R. E. Olson and R. B. Bernstein, J. Chem. Phys. **49**, 162 (1968); **50**, 246 (1969).
[g] R. G. Gordon, J. Chem. Phys. **41**, 1819 (1964).
[h] H. G. Bennewitz, K. H. Kramer, W. Paul, and J. P. Toennies, Z. Physik **177**, 84 (1964).

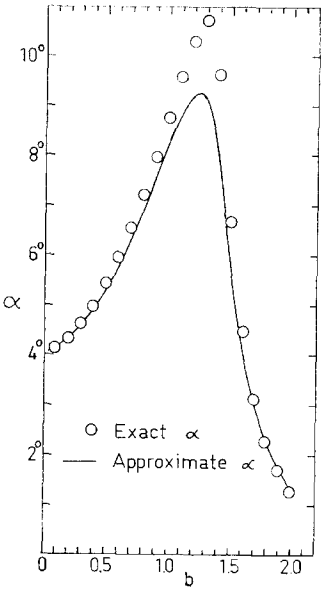

FIG. 20. Angle between initial and final rotational angular momentum vectors as a function of impact parameter.

figures when $\Delta j/j_0$ is small enough.[10] Inclusion of the Δ_2 term [Eq. (C8)] would not have significantly improved the agreement between exact and approximate results,[11] except in two of the figures—Fig. 11 for $I<0.01$ and Fig. 15 for $0.01<I<0.1$.

FURTHER REMARKS

It is seen from the figures that except in cases of low I (such as $HX+Y$, where $m_y \gg m_H$) the approximate Δj is a reasonably good one under the conditions investigated in the present paper. The source of the error at low I is not due to the approximation of replacing the relative translational motion by its elastic collision behavior since approximation 1 ("low mass") agrees well with the exact results there (Figs. 13–15).[12] Rather, it is probably due to replacing, in the zeroth-order behavior, the rotational motion by its unperturbed motion. That is, the present paper we have used in zeroth order the classical analog of the static approximation in quantum mechanics. Approximation 2(a) (in the direct calculation of Δj) provides a first-order calculation, one which corresponds in certain aspects to high order in the quantum case (in its allowance for the equivalent of many virtual-quantum jumps). Approximation 2(b) provides, with respect to reorientation of the plane of the rotor, the next higher order. At low I the distortion of the rotational motion may be large even in zeroth order, and one should then use some adiabatic approximation there instead.

Conditions where the present approximation for Δj is best correspond to some which are least accessible by approximate or numerical quantum mechanical methods. The expressions permit the ready investigation of various trends with molecular parameters.

The problem of treating rotation–translational energy transfer has sometimes been simplified by assuming the process to occur in a plane. It corresponds to the case where i_j in Fig. 1 (i_l in Fig. 3) is $\frac{1}{2}\pi$, and so its error can be estimated for various conditions at large enough I using (13)–(15).

In the evaluation of the relevant integrals in (13) and (15) use could not be made of an analytical technique frequently employed in vibrational–translational energy transfer. In the latter problem most of the transfer is usually assumed to occur over a small range of separation distance, where the perturbing force is large, permitting a simple analytical evaluation of the integrals by complex variable methods when those integrals are small. In the present case, over the range of parameters investigated, the transfer occurs over a large spatial region of perturbing force, so that it was not possible to apply such techniques.

The interpretation of many of the results in Figs. 4–20 was considerably simplified by defining the phases (in the angle variables) relative to the midpoint properties of the elastic collision, rather than as initial values.

APPENDIX A. DERIVATION OF EQ. (16)

We first compute Δj_x, Δj_y, Δj_z. We have

$$j_x = j \sin i_j \cos(\beta_{m_j} - \tfrac{1}{2}\pi),$$
$$j_y = j \sin i_j \sin(\beta_{m_j} - \tfrac{1}{2}\pi),$$
$$j_z = j \cos i_j. \tag{A1}$$

Thus,

$$\Delta j_x + i\Delta j_y = -i\Delta[j \sin i_j \exp(i\beta_{m_j})]. \tag{A2}$$

Evaluating Δj, Δi_j, and $\Delta\beta_{m_j}$ to first order by integrating (1), (3), and (4) one obtains Δj_x and Δj_y as the real and imaginary components of (A2). Δj_z is Δm_j obtained by integrating (2). Hence,

$$\Delta j_x = -\sin i_j \int_{-\infty}^{t} F \sin(\Phi' + \beta_{m_j}) \sin\psi dt, \tag{A3a}$$

$$\Delta j_y = \sin i_j \int_{-\infty}^{t} F \cos(\Phi' + \beta_{m_j}) \sin\psi dt, \tag{A3b}$$

$$\Delta j_z = -\cos i_j \int_{-\infty}^{t} F \cos\Phi' \sin\psi dt + \int_{-\infty}^{t} F \sin\Phi' \cos\psi dt. \tag{A3c}$$

From these values for Δj_x Δj_y, Δj_z, Δj can be computed as

$$\Delta j = [(j_x^0 + \Delta j_x)^2 + (j_y^0 + \Delta j_y)^2 + (j_z^0 + \Delta j_z)^2]^{1/2} - j_0. \tag{A4}$$

One obtains Δj represented by Eqs. (14), (13), and (15).

However, it is instructive to rewrite Δj_x, Δj_y, Δj_z in terms of components of $\Delta\mathbf{j}$ parallel to and perpendicular to $\mathbf{j}_0$. The parallel component is the projection of $\Delta\mathbf{j}$ and $\mathbf{j}_0$ and so equals

$$(j_x\Delta j_x+j_y\Delta j_y+j_z\Delta j_z)/j_0.$$

One then obtains (13) from (A3). Further,

Square of perpendicular component

$$=(\Delta j_x)^2+(\Delta j_y)^2+(\Delta j_z)^2-(\Delta j^{\|})^2. \quad \text{(A5)}$$

From (A2) and (A3), we have

$$(\Delta j_x)^2+(\Delta j_y)^2=|\Delta j_x+i\Delta j_y|^2$$
$$=\sin^2 i_j\left|\int_{-\infty}^{t} F\exp(i\Phi'+i\beta_{m_i})\sin\psi dt\right|^2. \quad \text{(A6)}$$

The $i\beta_{m_i}$ is next deleted without altering the right-hand side. Again, from Eq. (13) for $\Delta j^{\|}$ and (A3) for Δj_z one obtains

$$(\Delta j_z)^2-(\Delta j^{\|})^2=\sin^2 i_j\left[\left(\int_{-\infty}^{t} F\sin\Phi'\cos\psi dt\right)^2 - \left(\int_{-\infty}^{t} F\cos\Phi'\sin\psi dt\right)^2\right]. \quad \text{(A7)}$$

Introduction of (A6) and (A7) into (A5) yields (15).

APPENDIX B. INDIRECT CALCULATION OF Δj

Since l_x, l_y, l_z equal $l\sin i_l\cos(\beta_{m_l}-\frac{1}{2}\pi)$, $l\sin i_l\times\sin(\beta_{m_l}-\frac{1}{2}\pi)$, $l\cos i_l$, it can be shown from the equations for l, i_l, and β_{m_l} that

$$dl_x/dt=F(\gamma,t)\sin i_l\sin\Psi\sin\phi \quad \text{(B1)}$$

and

$$dl_y/dt=-F(\gamma,t)\sin i_l\sin\Psi\cos\phi. \quad \text{(B2)}$$

We have

$$(\Delta l_x)^2+(\Delta l_y)^2=|\Delta l_x+i\Delta l_y|^2$$
$$=\sin^2 i_l\left|\int_{-\infty}^{\infty} F(\gamma,t)\sin\Psi\exp i\phi\, dt\right|^2. \quad \text{(B3)}$$

Further, from the equation for $\dot{m}_l$ we have

$$\Delta m_l=\int_{-\infty}^{t} F(\gamma,t)(\cos i_l\cos\Psi\sin\phi'-\sin\Psi\cos\phi')dt. \quad \text{(B4)}$$

Comparison of Figs. 1 and 3 shows that i_j equals i_l; the γ's are also equal; ψ in Fig. 1 and ϕ' in Fig. 3 measure from the line of nodes the angle between the latter and the rotator's axis $\mathbf{r}$; Φ' in Fig. 1 and Ψ in Fig. 3 measure from the line of nodes between the latter and the line of centers of the collision partners $\mathbf{R}$. Thus, $\psi=\phi'$, $\Phi'=\psi$.

Comparison of (13) and (B4) then shows that they are equal. Further, the ϕ in the last term in (B3) may be replaced by ϕ' since multiplication of the integrand by $\exp(-i\beta_{m_l})$ leaves the term unchanged. Comparison of (B3) with (15) then shows that they are equal. Finally comparison of (18) with (14) then shows that they too are equal. Thus, the indirect calculation of Δj yields an expression which is identical with the calculation of Δj via (14).

APPENDIX C. DERIVATION OF EQ. (C7)

We use the notation $C(t)$ and $S(t)$:

$$C(t)=\int_{-\infty}^{t} F\cos\psi\sin\Phi' dt,$$

$$S(t)=\int_{-\infty}^{t} F\sin\psi\sin\Phi' dt, \quad \text{(C1)}$$

where all values on the right-hand sides denote elastic collision values. We denote by Δf the difference at time t of a quantity f from its elastic collision value. With the aid of (1), (2), and (5) one finds

$$\Delta\cos i_j=(\sin^2 i_j)C/j_0. \quad \text{(C2)}$$

Since the purpose of this appendix is to allow in the right-hand side of (1) for the change in rotational plane rather than for the change in j, we use the following results obtained from (3) and (4) at constant j,

$$\Delta\psi=(\cos i_j)S/j_0, \qquad \Delta\beta_{m_i}=-S/j_0. \quad \text{(C3)}$$

The quantities $\Delta(\cos\psi\sin\Phi')$ and $\Delta(\sin\psi\sin\Phi')$ are evaluated by expressing $\Delta[\exp(i\psi)\sin\Phi']$ in terms of $\Delta\psi$ and $\Delta\beta_{m_i}$, then using (C3), and finally recording the real and imaginary parts. Similarly, $\Delta(\cos\psi\cos\Phi')$ and $\Delta(\sin\psi\cos\Phi')$ are obtained by considering

$$\Delta[\exp(i\psi)\cos\Phi'].$$

One finds

$$\Delta\cos\psi\sin\Phi'=(\cos\psi\cos\Phi'-\cos i_j\sin\psi\sin\Phi')S/j_0, \quad \text{(C4a)}$$

$$\Delta\sin\psi\sin\Phi'=(\sin\psi\cos\Phi'+\cos i_j\cos\psi\sin\Phi')S/j_0, \quad \text{(C4b)}$$

$$\Delta\cos\psi\cos\Phi'=-(\cos\psi\sin\Phi'+\cos i_j\sin\psi\cos\Phi')S/j_0, \quad \text{(C4c)}$$

$$\Delta\sin\psi\cos\Phi'=(-\sin\psi\sin\Phi'+\cos i_j\cos\psi\cos\Phi')S/j_0. \quad \text{(C4d)}$$

Equations (C2) and the relevant portions of (C4) are next introduced into the right-hand side of (1), neglecting products of Δ's and later using the identity

$$G(t)\int_{-\infty}^{t} G(t')dt'=\frac{1}{2}\frac{d}{dt}\left[\int_{-\infty}^{t} G(t')dt'\right]^2. \quad \text{(C5)}$$

When products of ΔF and other Δ's are neglected one obtains

$$\frac{dj}{dt}=F(\cos i_j \cos\psi \sin\Phi'-\sin\psi \cos\Phi')+\frac{\sin^2 i_j[(d/dt)(S^2+C^2)]}{2j_0}, \quad \text{(C6)}$$

where all values on the right side, except the indicated F, are elastic collision values.

When both sides of (C6) are multiplied by j, higher-order terms neglected as before, an equation is obtained which can be rewritten as

$$j^2=(j_0+\Delta j^{\parallel})^2+\Delta_2+(\Delta j^{\perp})^2, \quad \text{(C7)}$$

where $\Delta j^{\parallel}$ and $(\Delta j^{\perp})^2$ are symbols denoting the right-hand sides of (13) and (15), respectively, and where

$$\Delta_2=2\int_{-\infty}^{t}\Delta F(\cos i_j \cos\psi \sin\Phi'-\sin\psi \cos\Phi')\,dt, \quad \text{(C8)}$$

and

$$\Delta F=(\partial F/\partial \cos\gamma)(\sin^2 i_j \sin\Phi')(C\sin\psi-S\cos\psi). \quad \text{(C9)}$$

Thus, apart from the Δ_2 term Eq. (14) allows (to second order in the j^2 expression) for the change in orientation of the rotational plane during the collision.

APPENDIX D. NUMERICAL INTEGRATIONS

Exact Δj

The exact results were obtained by numerically integrating the set of ten coupled differential equations in (D1) and (D2) from $R=R_{\text{initial}}$ through $R=R_{\min}$ to $R>R_{\text{initial}}$.

We have

$$\dot{X}_i=P_i/\mu, \quad \text{(D1a)}$$

$$\dot{P}_i=-(\partial V/\partial R)(X_i/R)-(\partial V/\partial \cos\gamma(\partial \cos\gamma/\partial X_i), \quad (i=1,2,3), \quad \text{(D1b)}$$

and

$$\dot{\theta}=P_\theta/I, \quad \text{(D2a)}$$

$$\dot{\phi}=P_\phi/I\sin^2\theta, \quad \text{(D2b)}$$

$$\dot{P}_\theta=-\partial V/\partial\theta+P_\phi^2\cos\theta/I\sin^3\theta, \quad \text{(D2c)}$$

$$\dot{P}_\phi=-\partial V/\partial\phi. \quad \text{(D2d)}$$

Here,

$$\cos\gamma=X_1\sin\theta\cos\phi+X_2\sin\theta\sin\phi+X_3\cos\theta.$$

The X_i are the cartesian components of R, while the P_i are their conjugate momenta. A coordinate system similar to the one in Fig. 3 was used so that initially $\sin\theta=1$, and $\sin\theta$ could only become small if $\mathbf{j}$ rotated through approximately $\frac{1}{2}\pi$ during the collision. Initial values of t and Ψ in Fig. 3 were obtained by integrating the equations (D3) for elastic orbital motion from $R=R_{\min}$ to $R=R_{\text{initial}}$.

We then have,

$$\dot{R}=P_R/\mu,$$
$$\dot{\Psi}=l_0/\mu R^2,$$
$$\dot{P}_R=-\partial V_0/\partial R. \quad \text{(D3)}$$

Here, V_0 equals $V-V_p$ in (9) or (19). $R_{\min}$ was determined by numerically estimating the largest root of the function in brackets in Eq. (12).

Nordsieck's integration method[13] was used to evaluate the sets of coupled differential equations. Both total energy and angular momentum were normally conserved to better than a few hundredths of a percent. Test collisions integrated using seven[4] rather than ten differential equations yielded the same result to five significant figures.

Flywheel and Low Mass Δj

The flywheel solution (indirect approximation 1) was obtained by integrating the six coupled differential equations in (D1) using Nordsieck's method.[13] The elastic values for rotational motion ($\theta=\frac{1}{2}\pi$, $\phi=j_0t/I+\phi_{\text{initial}}$) were used. Then the flywheel Δj was obtained from $\Delta\mathbf{l}$ using conservation of total angular momentum ($\Delta\mathbf{j}=-\Delta\mathbf{l}$).

The low mass solution (direct approximation 1) was obtained by integrating the seven differential equations in (D2) and (D3) using Nordsieck's method.[13] Computer times for calculating the exact, flywheel, and low mass solutions were comparable.

$\Delta j^{\parallel}$ and Approximate Δj

For the potential in Eqs. (19) and (20), $\Delta j^{\parallel}$, Δm_j, $\Delta\beta_{m_j}$, and $\Delta j^{\perp}$ can be expressed in terms of five integrals.

We have, for example,

$$\Delta j^{\parallel}=2F_2\sin^2 i_j\sin 2\phi^r-F_4(1-\cos i_j)\sin\phi^+ +F_5(1+\cos i_j)\sin\phi^-, \quad \text{(D4)}$$

where

$$F_1=\frac{3}{4}\int_0^\infty V_{RA}\,dt,$$

$$F_2=\frac{3}{4}\int_0^\infty V_{RA}\cos(2\omega_0 t)\,dt,$$

$$F_3=\frac{3}{4}\int_0^\infty V_{RA}\cos 2\bar{\Phi}\,dt,$$

$$F_4=\tfrac{3}{4}(1-\cos i_j)\int_0^\infty V_{RA}\cos(2\omega_0 t+2\bar{\Phi})\,dt,$$

$$F_5=\tfrac{3}{4}(1+\cos i_j)\int_0^\infty V_{RA}\cos(2\omega_0 t-2\bar{\Phi})\,dt. \quad \text{(D5)}$$

Here,

$$V_{RA}=4\epsilon[a_R(R/\sigma)^{-12}-a_A(R/\sigma)^{-6}],$$

$$\Phi=\int_0^t \frac{l_0}{\mu R^2}\,dt,$$

$$\phi^+=2\phi^R+2\phi^r,$$

$$\phi^-=2\phi^R-2\phi^r,$$

$$\omega_0=j_0/I.$$

The integrals determining $\Delta j^{\perp}$ in Eq. (15) are also easily expressed in terms of the F_i:

$$\int_{-\infty}^{+\infty} F(\gamma,t)\,\sin\Phi'\cos\psi dt=-2F_2\cos i_j\sin 2\phi^r$$

$$-2F_3\sin\phi^R+F_4\sin\phi^++F_5\sin\phi^-,$$

$$\int_{-\infty}^{+\infty} F(\gamma,t)\,\sin\Phi'\sin\psi dt=-2F_1\cos i_j-2F_2\cos i_j\cos 2\phi^r$$

$$-2F_3\cos i_j\cos 2\phi^R+F_4\cos\phi^+-F_5\cos\phi^-. \quad \text{(D6)}$$

The approximate Δj was calculated from Eqs. (14), (15), and (D4)–(D6).

The integrals in (D5) were evaluated numerically by using Nordsieck's method[13] to integrate the set of eight differential equations consisting of the ones in (D3) and the five equations for dF_i/dt ($i=1$–5) obtained from (D5).

APPENDIX E. MISPRINTS IN PART I

Part I contains a number of misprints made in transcribing the results from Ref. 1 there to Part I:

In Eq. (6) *for* $m_l\csc^2\Theta$ *read* $m_l^2\csc^2\Theta$; in (15) and (17) the minus sign should be deleted, as should the first minus sign in the top line of Eq. (22). In (16) and (18) the symbols ϕ and Φ should be interchanged. In (31) *for* $\mu/2$ *read* $2/\mu$. Both in Fig. 1 and in the paragraph preceding (20) the $+\frac{1}{2}\pi$ should be replaced by $-\frac{1}{2}\pi$, wherever it appears.

In Ref. 17 it should have been added that ultimately, in obtaining (14) to (18) there, the negative square root sign was selected.

* Acknowledgment is made to the National Science Foundation and to the donors of the Petroleum Research Fund, administered by the American Chemical Society, for their support of this research.

† Present address: International Business Machines, Cambridge, Mass.

[1] A. O. Cohen and R. A. Marcus, J. Chem. Phys. **49**, 4509 (1968). A number of misprints are listed in Appendix E of the present paper. For use of local action-angle variables in certain chemical reactions see R. A. Marcus, J. Chem. Phys. **49**, 2617 (1968).

[2] R. A. Marcus, (unpublished). For use of exact classical results to interpret quantum approximations in a vibrational–translational problem see M. Attermeyer and R. A. Marcus, J. Chem. Phys. **52**, 393 (1970).

[3] When the xy plane is chosen for the orbital plane in elastic collision, $\Theta=\frac{1}{2}\pi$, $p_\Theta=0$, $p_\Phi=l$, the orbital angular momentum. The differential equations for R, Θ, Φ, p_R, p_Θ, p_Φ then yield on integration Eqs. (11) and (12) of the present paper. The latter, expressed as the two differential equations,

$$\dot{\Phi}=l_0/\mu R^2,\ \dot{R}=\{2[E-V_0-E_{\rm rot}-(l_0^2/2\mu R^2)]/\mu\}^{1/2},$$

and the four rotator differential equations [Eq. (26) of Part I] are integrated numerically, as discussed in Appendix D.

[4] For example, L. C. Biedenharn and P. J. Brussard, *Coulombic Excitation* (Oxford University Press, Oxford, England, 1965), p. 32ff. T. M. Cottrell and J. C. McCoubrey, *Molecular Energy Transfer in Gases* (Butterworths Scientific Publications Ltd., London, 1961), Chap. 6.

[5] R. J. Cross and D. R. Herschbach, J. Chem. Phys. **43**, 3530 (1965).

[6] P. W. Anderson, Phys. Rev. **76**, 647 (1949); J. I. Gersten and H. M. Foley, *ibid.* **182**, 24 (1969), and references cited therein.

[7] For example, R. G. Gordon, W. Klemperer, and J. I. Steinfeld, Ann. Rev. Phys. Chem. **19**, 215 (1968), Table I.

[8] Whenever comparison with Eq. (14) is referred to in text, it is understood that the $\Delta j^{\parallel}$ and $(\Delta j^{\perp})^2$ appearing in it are given by (13) and (15), respectively.

[9] T. M. Apostol, *Mathematical Analysis* (Addison–Wesley Pub. Co., Inc., Reading, Mass., 1957), p. 469.

[10] Specifically, this occurs in Fig. 7 when $a_2<0.4$, in Fig. 9 when $E^R>1.0$ ($b=0.4$) and when $E^R>2.0$ ($b=1.0$), in Fig. 10 when $E^r>0.05$ ($b=0.1$) and $E^r>0.2$ ($b=1.0$), in Fig. 12 when $I>0.5$, in Fig. 13 when $I>0.5$, in Fig. 14 when $I>0.1$, in Fig. 16 when $b>1.0$ ($a_A=0$, $a_R=0.3$) and when $b>1.2$ ($a_A=0.3$, $a_R=0$), in Fig. 17 when $j_0>5\hbar$, in Fig. 18 when $j_0>3\hbar$, and in Fig. 19 when $j_0>70\hbar$.

[11] This lack of improvement prevails because Δ_2 becomes vanishly small as the angular frequency of rotation ω becomes small or becomes very large. Hence, to improve results by including Δ_2, a case must be selected with ω in a narrow range and yet with I and E^r such that the first-order $\Delta j^{\parallel}$ is beginning to fail. As far as numerical evaluations are concerned, more computer time is required to evaluate Δ_2 than to evaluate the exact Δj.

[12] Within the framework of the discussion in Appendix C one principal source of error at low I may be the neglect in Eq. (C3) of a term involving a Δj in the expression for $\psi(t)$. The modified expression for ψ would be $\int\omega(t)dt$, where $\omega(t)$ reduces to ω at large $|t|$.

[13] A. Nordsieck, Math. Computation **16**, 22 (1962); H. R. Lewis, Jr. and E. J. Stovall, Jr., Math. Computation **21**, 157 (1967).